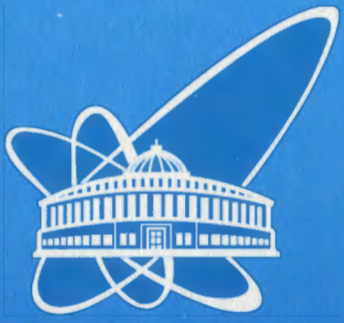

ОБЪЕДИНЕННЫЙ
ИНСТИТУТ
ЯДЕРНЫХ
ИССЛЕДОВАНИЙ

Дубна

E1-2000-307

V.P.Bamblevski, A.R.Krylov, A.Polanski,
G.N.Timoshenko, V.N.Shvetzov

# THE INVESTIGATION OF THE RADIATION FIELD AROUND THE THICK LEAD TARGET IRRADIATED BY THE 650 MeV PROTONS

## Part 1. The Neutron Spectra Measurement around the Target

Submitted to «Nuclear Instruments and Methods A»

2000

In the frame of the project SAD (MOX subcrutical assembling in Dubna) /1/ the first stage of the experimental investigation was carried out at the LNP Phasotron. The main object of this experiment was to study the differential characteristics of the secondary radiation field around the thick target irradiated by the protons. The target imitates the core of the subcritical assembling. Such experimental data are needed for verification of the calculations of the internuclear cascade of the secondary particles generated by the primary protons within the target.

Two main types of the characteristics of the radiation field were investigated during the experiment:

- the double differential (angle and energy) distribution of the neutrons escaped from the target;
- the angle and spatial distributions of the hadron (neutron, proton, $\pi$-meson) yield from the target and the total yield of the hadrons from the target.

In the present paper the general conditions of the experiment and the technique of the neutron spectra measurements are described.

## EXPERIMENTAL SET-UP

The target was assembled from four equal cylinders of natural lead (each of 12.5 cm lengthwise and 8.2 cm in diameter) covered by the 1,5 mm layer of stainless steel. The target was mounted within the cabin № 7 (Fig.1) of LNP clinical-physical complex /2/. The proton beam extracted from the Phasotron with timing stretching passed then through the narrow collimator of the carbon absorber for reduction of the initial proton current (~0.2 $\mu$A) down to the intensity of $10^9 \div 10^{10}$ $s^{-1}$. Then the proton beam was focused on the centre of the target by the couple quadrupole magnetic lenses ML-7, ML-8. The

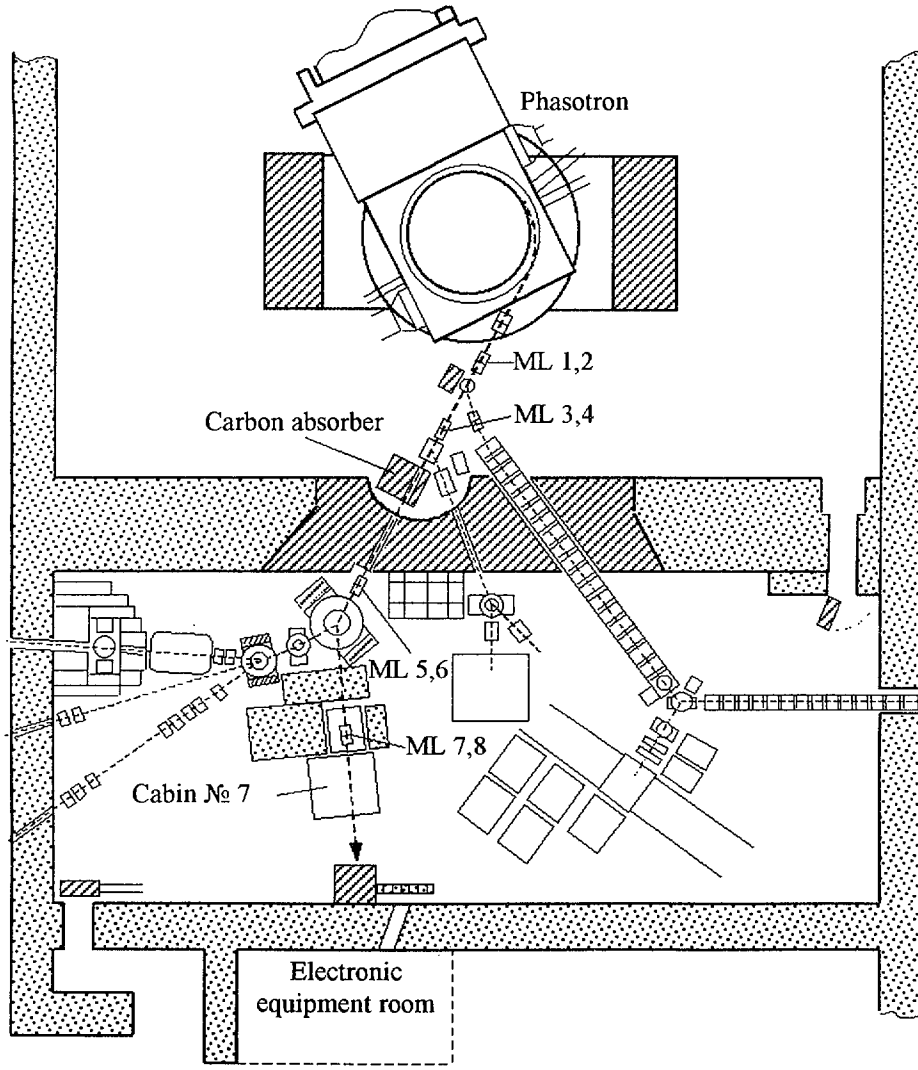


Fig. 1 The general experimental layout

spatial distribution of the protons in front of the target was measured by the matrix of the thermoluminescent detectors (HARSOW TLD-600). The TLD size was 3.1 × 3.1 $mm^2$ and the thickness was 0.9 mm. We used the matrix from 15×9=135 TLD spaced in 6 mm one after another (whole matrix dimensions are 8.8 (X) × 5.2 (Y) $cm^2$). In order to decrease the TLD sensitivity dispersion the matrix graduation with $^{60}Co$ was carried out preliminarily. The individual correction coefficient for each detector was obtained and then it was taken into account during the data processing. The spatial distribution of the protons measured by the TLD matrix (in term of nC) is presented in Fig. 2. The average standard deviation of the proton flux distribution was estimated as 4.2 mm.

For the absolute monitoring of the protons interacting with the target the thin ionization chamber (25 cm in diameter) was placed in 30 cm up-stream the target. The chamber current went through the short cable to the current-frequency converter with sensitivity 37.5 $imp \cdot nC^{-1}$. The current-frequency converter calibration with the direct current source showed that up to $10^5$ $imp \cdot s^{-1}$ rate its integral nonlinearity was less than 0.2%.

The absolute calibration of the beam current chamber was carried out with the thin carbon-contained activation detectors (10 cm in diameter) placed directly on the chamber surface. The calibration procedure was repeated four times at the different beam intensities within the real beam intensity range. The detector activities were measured by the gamma-spectrometer very thoroughly with account of the real source-detector geometry and the self-absorption process. The cross section of the $^{12}C(p, pn)^{11}C$ reaction was taken equal to 30.5 ± 1 mb. The resulting error of the proton flux measurements was estimated as 5÷6 % (including the reaction cross section error, methodological and statistical errors and taking into account the time structure of irradiation). We tested the linearity of the chamber readings depending on the beam intensity in the working range (Fig.3). Finally, the chamber conversion factor was defined as $6.18 \times 10^5$ $proton \cdot imp^{-1}$.

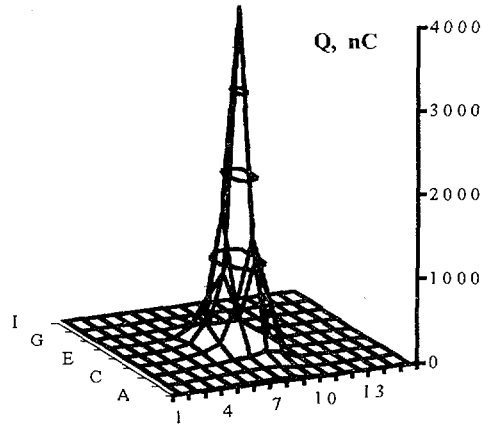


Fig. 2. The spatial distribution of the TLD matrix responses.

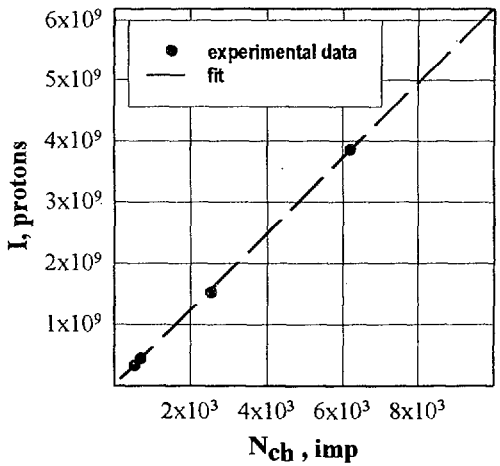


Fig.3. The beam current chamber calibration.

## THE NEUTRON SPECTRA MEASUREMENT

The measurement of the double differential (angle and energy) distribution of the neutrons generated in the target is a difficult problem due to the widest energy range and the complex background condition mainly. Most of the well-known techniques of the neutron spectrum measurement can be applied within relative narrow energy ranges overlapping the various parts of the spectrum only. There are also the other difficulties in use of these methods in the experiment (its low sensitivity or selectivity, the angular dependence etc.). As a result, the multisphere technique for measurement of the neutron spectra in mixed radiation field around the lengthy target was chosen as the first step of this investigation. It should be marked that this technique is not practically used in the physics experiments with targets, but it is the basic tool of the investigations in mixed scattered radiation fields in the radiation protection physics.

The proposed technique has both advantages and imperfections. The advantages are the very wide energy range (from the thermal energy to the energy of initial protons), the insensitivity for charged particles and good selectivity for gamma rays, the angular anisotropy and the simplicities of the instrument and of the measurement procedure. The imperfections of the method are the complexity of the neutron spectra unfolding (using special mathematical methods) and poor information in the energy region above several tens of MeV (that is connected with the near linear dependence of the spectrometer response functions in the high-energy region).

The multisphere neutron spectrometer (SB) on the basis of the LiI(Eu) crystal (4 mm in height and 4.3 mm in diameter) enriched by $^{6}$Li up to 90% and coupled with the spectrometric photomultiplier was used with the set of the polyethylene spherical moderators of 2, 3, 5, 7, 8, 10, 12 inches in diameter. The spectrometer was connected through the cable with the multichannel analyzer on PC basis. The apparatus spectrum from LiI(Eu) crystal presents the narrow peak caused by the $^{3}$He and $^{3}$H detection ($^{6}$Li+n = $^{3}$He+$^{4}$He reaction) and is

placed on the falling background spectrum of the gamma rays. The neutron spectra unfolding is the solution of the Fredholm integral equation system (the 2-nd kind):

$$N_i = \int_{E_{min}}^{E_{max}} F(E) \cdot \varphi_i(E) \cdot dE \qquad (1)$$

where $F(E)$ – the neutron flux ($cm^{-2} \cdot s^{-1}$) depending on the energy in the place of the sphere position, $\varphi_i(E)$ – the response function of $i$-sphere ($cm^2$), $N_i$ – the $i$- sphere's reading ($s^{-1}$). At present, there is the set of the SB response functions calculated by the different authors, but the most precise calculation of the functions and its experimental verification in wide energy range was carried out in the frame of the European Commission contract /3/. These response functions for the above-mentioned spheres were calculated by MCNP code up to energy of 20 MeV. For the highest neutron energy (up to 1.5 GeV) the calculation was continued by the HADRON code /4/. Unfortunately, the experimental test of the SB response function calculation in the energy range over 14 MeV was not carried out. The design of our SB and the SB used in /4/ slightly differs. Because of it, the preliminary calibration of our SB response functions for all spheres was done with a standard $^{252}Cf$ source with the neutron yield known within 5% accuracy. The obtained coefficients were used then for the regulation of the SB readings. The neutron spectrum unfolding was carried out by the statistical regularization method with attraction of a priori information about the spectrum shape /5/. As a priori information, the assumptions about the smoothness of the neutron spectrum and the absence of the neutrons with the energy above the initial proton energy were used. The errors of the unfolded spectrum are the standard deviation of the spectrum function at the given neutron energy. As the neutron spectrum spreads often on several decades of energy, the spectrum presentation in the energy lethargy term is usually used.

## RESULTS AND DISCUSSION

The experimental arrangement is presented in Fig.4. The neutron spectra measurements were carried out under the angles $45^0$, $75^0$ and $105^0$ to the beam direction. The distance between the SB and the target as well as the proton beam intensity were chosen from the requirement of smallness of the SB miscounts. Under the distance 2.77 m the spectrometer miscounts were less than 1%; the maximum angle resolution (for the 12″ sphere) was $\pm$ $3.2^0$ and the maximum solid angle was $9.6 \cdot 10^{-3}$ sr.

The scattered neutron background in the experimental place was due to two sources mainly: the first was the leakage neutrons from the shielding between the experimental hall and the cyclotron and the second was the neutrons from the target scattered within the experimental hall. For the subtraction of the scattered neutron background from the SB readings the separate measurements with the shadow bar were carried out under every angle. For the reliable neutron spectra unfolding the differences of the normalized $N_i$ between both types of measurements were used as the left parts of the equation system (1). The mobile shadow bar was constructed from the still blocks (total thickness was 30 cm) mounted on the frame. The distance between the target and the bar centre was 2 m and the bar cross-section was recovering the target projection wholly (see Fig.4). The background count rates at given experimental conditions were very high and for the different spheres the background counts varied from ~ 85 % (2″ sphere) up to ~ 35 % (12″ sphere). Such background levels were approximately constant under all angles.

Unfortunately, the bar thickness was insufficient for the reliable elimination of the neutrons from the target. The following calculation by the MCNP code with the real geometry was done for the estimation of the SB counts produced by the leakage neutrons from the shadow bar ($N_i'$) and by the direct neutrons from the target ($N_i$). As the neutron source was taken, in the first approach, the part of the unfolded neutron spectrum under $75^0$ with upper border 100 MeV (more than 95% of the total neutron fluence). In Fig.5 the calculated

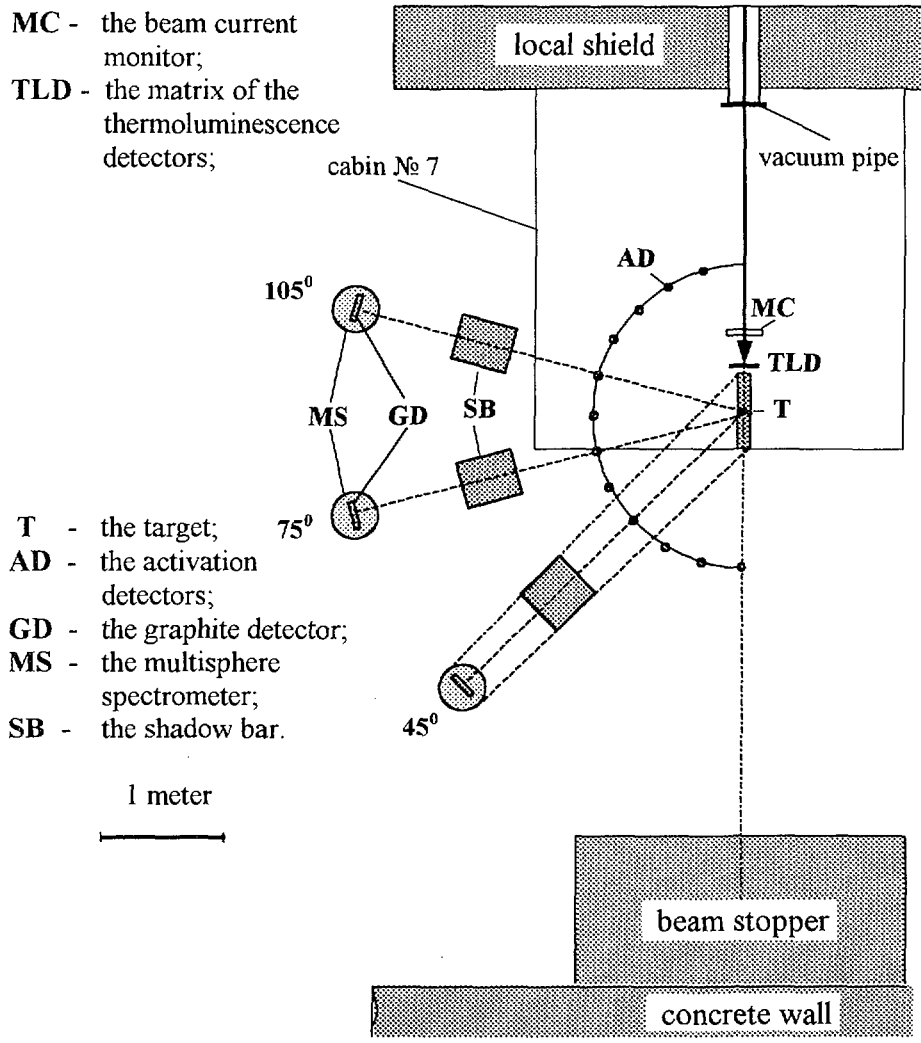


Fig.4 The arrangement of the experiment

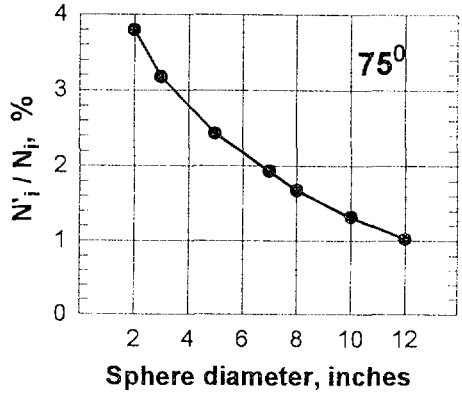


Fig.5. The contribution of the SB counts from the neutrons penetrated through the shadow bar ($N'_i$) to the SB counts from the initial neutrons ($N_i$).

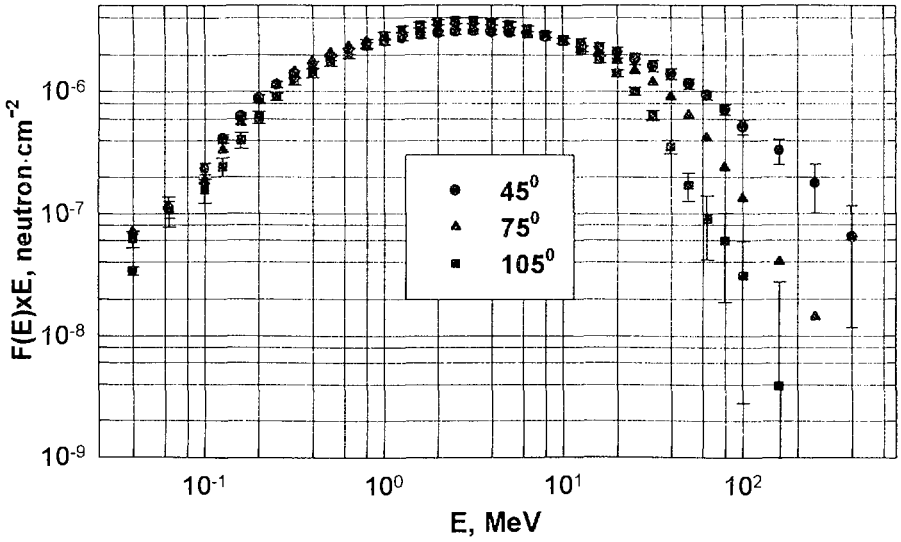


Fig.6. The neutron spectra from the target

relation between these SB counts (in %) depending on the spheres diameter is presented. The calculation showed that due to this effect the resulting subtraction of the background by the shadow bar was overestimated on the 2-3% maximum.

Besides the SB data, the results of measurements with the activation detectors were included in the equation systems (1) for the improvement of the unfolding of the high-energy parts of the neutron spectra. As the activation detector the graphite disks with 13 cm of diameter and 1.8 cm of thickness were used. The cross-section of the $^{12}C(n, 2n)^{11}C$ reaction with the threshold about 20 MeV is known with the 5% error within the analyzed energy range. The admixture of the charged hadrons from the target was insignificant, and the total detector activation considered in the given case as produced by the neutrons. The detector activity measurements were done with the low background gamma-spectrometer at once after the detectors irradiation. The activation detector equation had the following form:

$$A^{\infty} / M_d = \int_{E_{min}}^{E_{max}} F(E) \cdot \sigma(E) \cdot dE$$

where $\sigma(E)$ – the reaction cross-section ($cm^2$), $A^{\infty}$ - the detector's activity extrapolated to the infinite time of the irradiation ($s^{-1}$), $M_d$ – the total amount of $^{12}C$ atoms in the detector. The "transparence" of the detector for the high-energy neutrons had been preliminary confirmed by the MCNP code calculation, therefore the use of the $\sigma(E)$ in the right part of the equation was valid enough. The activation detectors were irradiated behind the shadow bar under every angle just as the SB spheres.

The unfolded neutron spectra are shown in Fig. 6. All results are normalized to the target irradiation by one proton. The presented spectra are the fluence energy dependences (averaging on the spheres volumes) in the points of the spheres positions. Such presentation, by our opinion, is more correct than it would be in the terms of the neutron yield energy dependences from the target in unit solid angle. The fluences of the neutrons under all angles are differed a little that is caused by the target geometry (its length is much larger than the

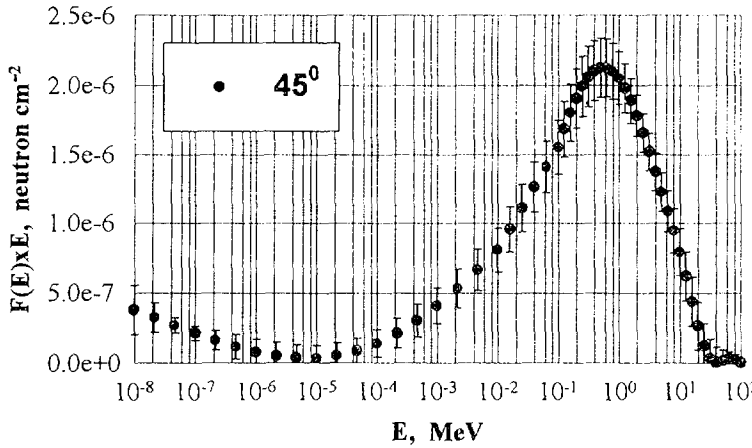


Fig. 7. The background neutron spectrum.

proton's range). The main parts of the spectra are owing to the neutrons many times scattered (by the inelastic manner mainly) within the target. The epithermal and intermediate neutrons are practically absent in the spectra. The lower energy borders of the fast neutrons and the spectra shapes up to the energy of 10 MeV are practically identical. The main spectra characteristics normalized to 1 beam proton are given in Table 1.

Table 1.

| Angle (deg.) | 45 | 75 | 105 |
|---|---|---|---|
| Fluence ($n \cdot cm^{-2}$) | $(1.40 \pm 0.05) \cdot 10^{-5}$ | $(1.42 \pm 0.06) \cdot 10^{-5}$ | $(1.26 \pm 0.07) \cdot 10^{-5}$ |
| Average energy (MeV) | 14.9 | 7.6 | 5.7 |
| Fluence >20 MeV (%) | 17.1 | 9.3 | 5.4 |

The coincidence of the real $N_i$ and $N_i$ obtained with the unfolding spectrum is only one formal criterion of the accuracy of the spectrum unfolding. For the presented spectra the differences between these $N_i$ do not exceeded 8%, typically. The consequence of the assumption about smoothness of the neutron spectrum as a priori information at the spectrum unfolding can be slight expansion and flatness of the spectrum (depending on the class of the spectral function). For the present spectra shape, it was checked by the "paper" experiment with the assigned testing spectrum, having the shape similar to the real neutron spectrum. The test shows that for the unfolded spectra their expansions are negligible.

In Fig. 7 the average background neutron spectrum behind the shadow bar is presented (the background spectra under all angles have the similar form and the flux). The spectral shape is evidence of two different sources of the background neutrons. The soft part of the spectrum is caused by the leakage neutrons from the Phasotron shield. Owing to the absence of significant mass of any hydrogen-contained matter in the experimental hall the epithermal part of the background spectrum is suppressed. The peak of the fast neutrons in the spectrum is produced by the neutrons from the target scattered in the experimental hall and by the small portion of the neutrons passed through the shadow bar. The average background neutron fluence

behind the bar was $(1.44\pm0.04)\cdot10^{-6}$ neutron·cm$^{-2}$ per 1 proton coming in the target, but only 15.5% of all background neutrons had the energies over 0.1 MeV and overlaped the neutron spectra from the target.

This work was carried out by the partial financial support of the Forschungszentrum Karlsruhe, contract № 315/20171212/IKET

REFERENCES

1. V.S.Barashenkov, A.Polanski, I.V.Puzynin, A.N.Sissakian. An Experimental Accelerator Driven System Based on Plutonium Subcritical Assembly and 660 MeV Proton Accelerator. Proc. 3rd Int. Conf. On Accelerator Driven Transmutation Technologies and Application, June 7-11, 1999, Prague, Czech Republic (CD-ROM edition). Preprint JINR E2-99-207, Dubna, 1999.

2. O.V.Savchenko. Preprint JINR E18-96-124, Dubna, 1996.

3. M.Kralik, A.Aroua, M.Grecescu, V.Mares, T.Novotny, H.Shraube and B.Weigel. Specification of Bonner Sphere Systems for Neutron Spectrometry. Radiat. Protect. Dosim. Vol. 70, No. 1- 4, pp. 279-284 (1997).

4. A.V.Sannikov, V.Mares and H.Shraube. High Energy Response Functions of Bonner Spectrometers. Radiat. Protect. Dosim. Vol .70, No. 1-4, pp. 291-294 (1997).

5. A.R.Krylov, G.N.Timoshenko, V.E.Aleinikov. Neutron Spectra in the Energy Range from $10^{-8}$ to Hundreds of MeV Measurement in Hard Scattered Radiation Field. JINR Communication P16-91-177, Dubna, 1991 (in Russian).

Received by Publishing Department
on December 21, 2000.